Search for 2β decay of cadmium and tungsten isotopes: Final results of the Solotvina experiment

F. A. Danevich, A. Sh. Georgadze, V. V. Kobychev, B. N. Kropivyansky, A. S. Nikolaiko, O. A. Ponkratenko, V. I. Tretyak, S. Yu. Zdesenko, and Yu. G. Zdesenko*
Institute for Nuclear Research, MSP 03680 Kiev, Ukraine

P. G. Bizzeti, T. F. Fazzini, and P. R. Maurenzig
Dipartimento di Fisica, Universitá di Firenze and INFN, 50019 Firenze, Italy
(Received 21 March 2003; published 4 September 2003)

Final results of the double β decay experiment, performed with the help of low background $^{116}CdWO_4$ crystal scintillators in the Solotvina Underground Laboratory, are presented. In particular, the revised half-life value of the two-neutrino 2β decay of ^{116}Cd has been measured as $T^{2\nu}_{1/2}=2.9^{+0.4}_{-0.3}\times10^{19}$ yr, and the new half-life limit on the neutrinoless 2β decay of ^{116}Cd has been established as $T^{0\nu}_{1/2}\geqslant1.7(2.6)\times10^{23}$ yr at 90% (68%) C.L. The latter corresponds to a restriction on the neutrino mass: $m_\nu\leqslant1.7(1.4)$ eV at 90% (68%) C.L. Besides, new $T_{1/2}$ bounds (at the level of 10^{17}–10^{21} yr) were set for various 2β processes in ^{106}Cd, ^{108}Cd, ^{114}Cd, ^{180}W, and ^{186}W nuclei.

DOI: 10.1103/PhysRevC.68.035501 PACS number(s): 23.40.−s, 27.60.+j, 27.70.+q, 29.40.Mc

I. INTRODUCTION

Recent observations of neutrino oscillations [1–4] provide important motivation for double beta (2β) decay experiments [5–7]. Indeed, the neutrinoless (0ν) mode of 2β decay, which violates lepton number (L) conservation and requires the neutrino to be a massive Majorana particle, is forbidden in the framework of the standard model (SM) of electroweak theory. However, many extensions of the SM incorporate L violating interactions and, thus, could lead to this process, which, when observed, would prove the Majorana nature of the neutrino. Hence, the discovery of the $0\nu2\beta$ decay would be a clear evidence for a new physics beyond the SM [5–7]. Moreover, while oscillation experiments are sensitive to the neutrino mass difference, the measured $0\nu2\beta$ decay rate can give the absolute scale of the effective Majorana neutrino mass and test different neutrino mixing models.

Despite numerous experimental efforts this process still remains unobserved, and only half-life limits for 0ν mode have been obtained in direct experiments up to now (see reviews in Refs. [5–8]). The highest bounds have been established for several nuclides: $T^{0\nu}_{1/2}\geqslant10^{21}$ yr for ^{48}Ca [9], ^{150}Nd [10], ^{160}Gd [11], ^{186}W [12]; $T^{0\nu}_{1/2}\geqslant10^{22}$ yr for ^{82}Se [13], ^{100}Mo [14]; $T^{0\nu}_{1/2}\geqslant10^{23}$ yr for ^{116}Cd [15], ^{128}Te, ^{130}Te [16] , ^{136}Xe [17]; and $T^{0\nu}_{1/2}\geqslant10^{25}$ yr for ^{76}Ge [18,19].

In the present paper we describe the final results of the ^{116}Cd 2β decay studies, which have been performed by using cadmium tungstate crystal scintillators (with natural isotopic composition crystals and ones enriched in ^{116}Cd to 83%) in the Solotvina Underground Laboratory [20] since 1988 [21]. The results obtained on the different phases of these researches have been published earlier [21–28,15,29,12]. The Solotvina experiment has been stopped in July 2002.

*Corresponding author. Email address: zdesenko@kinr.kiev.ua

II. EXPERIMENT AND DATA ANALYSIS

A. The low background setup

Description of the last modification of the setup with cadmium tungstate ($CdWO_4$) crystal scintillators and its performance have been already published [15], thus only the main features of this apparatus are summarized here. The experiment was carried out in the Solotvina Underground Laboratory at a depth of 1000 m of water equivalent [20]. The $^{116}CdWO_4$ crystal scintillators, enriched in ^{116}Cd to 83%, have been grown for the search [21]. Their light output is $\approx$30–35% as compared with that of NaI(Tl). The fluorescence peak emission is at 480 nm with principal decay time of ≈13 μs. Four $^{116}CdWO_4$ crystals with a total mass of 330 g were used in the setup. These are viewed by a low background 5″ EMI D724KFL photomultiplier (PMT) through one light guide 10 cm in diameter and 55 cm long. The light guide consists of two parts: high purity quartz (25 cm) and plastic scintillator (30 cm). The $^{116}CdWO_4$ crystals are surrounded by an active shield made of 15 $CdWO_4$ crystals of large volume with a total mass of 20.6 kg [30,31]. These are viewed by a low background PMT through an active plastic light guide 17 cm in diameter and 49 cm long. The whole $CdWO_4$ array is situated within an additional active shield made of plastic scintillator $40\times40\times95$ cm, thus, together with both active light guides, a complete 4π active shield of the main ($^{116}CdWO_4$) detector is provided. The outer passive shield consists of high purity copper (3–6 cm), lead (22.5–30 cm), and polyethylene (16 cm). Two plastic scintillators ($120\times130\times3$ cm) installed above the passive shield serve as cosmic muon veto.

The event-by-event data acquisition is based on two personal computers (PC) and a CAMAC crate with electronic units. For each event within the ^{116} $CdWO_4$ detector array, the following information is stored on the hard disk of the first PC: the amplitude of a signal (in the energy range of 0.12–5.4 MeV), its arrival time, and additional tags [the coincidence between the main and shielding detectors; triggers for a light emitting diode (LED) and for the transient digi-

tizer]. The second PC records the pulse shape (2048 channels, each of 50 ns width) of the $^{116}CdWO_4$ signals in the energy range 0.3–5.4 MeV (in special runs, the threshold was set at 80 keV) by using the transient digitizer (based on a 12-bit analog-to-digital converter Analog Devices AD9022) connected to the PC by a parallel digital board [32].

The energy scale and resolution of the $^{116}CdWO_4$ spectrometer were determined with various γ sources (^{22}Na, ^{40}K, ^{60}Co, ^{137}Cs, ^{207}Bi, ^{226}Ra, ^{232}Th, and ^{241}Am). The energy dependence of the resolution in the energy interval 60–2615 keV is expressed as follows: $\mathrm{FWHM}_\gamma = -44 + \sqrt{2800 + 23.4E_\gamma}$, where energy E_γ and FWHM_γ are in keV. For instance, energy resolutions of 33.7%, 13.5%, 11.5%, and 8.0% were measured for γ lines with energies of 60, 662, 1064, and 2615 keV, respectively. Routine calibrations were carried out with ^{207}Bi and ^{232}Th γ sources. The stability of the spectrometer is demonstrated by the fact that resolution of the ^{137}Cs peak in the background spectra (collected over 13 316 hours) is FWHM $\approx$14%, which is practically the same as measured in the calibration runs. The dead time of the detector and data acquisition was permanently controlled with the help of a light emitting diode optically connected to the main PMT (typical value was about 4%).

Besides, the relative light yield for α particles as compared with that for β particles (γ rays) with the same energies (so-called α/β ratio, which can be defined as the ratio of the energy of α particles measured in the γ scale of the detector, E_α^γ, to their actual energy, E_α) was determined in the energy range of 2.1–8.8 MeV. First, a collimated beam of α particles from ^{241}Am source penetrated through the thin absorbers with known thicknesses was used. The energy of the α particles after the absorber was accurately calculated and was also measured by a surface-barrier detector (we refer for details to work [33]). Second, the α peaks from the intrinsic trace contamination of the $^{116}CdWO_4$ crystals by nuclides of the Th chain (selected by the time-amplitude and the pulse-shape analysis as described below) were also utilized for the α/β ratio determination. In addition, we found the dependence of the α/β ratio (and pulse shape as well) on the direction of α particles beam relative to the main crystal axes [33]. Finally, it yields $\alpha/\beta = 0.083(9) + 1.68(13) \times 10^{-5} E_\alpha$, and $\mathrm{FWHM}_\alpha^\gamma(\mathrm{keV}) = 33 + 0.247E_\alpha^\gamma$, where E_α and E_α^γ are in keV.

Due to the active and passive shields, and as a result of the time-amplitude and the pulse-shape analysis of the data (see below), the background rate of the $^{116}CdWO_4$ detector in the energy region 2.5–3.2 MeV ($0\nu2\beta$ decay energy of ^{116}Cd is 2.8 MeV) is reduced to 0.04 counts/(yr kg keV). It is the lowest background rate which has ever been reached with crystal scintillators.

B. Pulse-shape discrimination technique

According to the measured α/β ratio, α particles from uranium and thorium trace contamination of the crystals can produce a background in the 0.4–1.3 MeV energy region, while overlapping of the β and α signals from two fast sequential decays, e.g., ^{212}Bi ($Q_\beta = 2.25$ MeV) $\rightarrow$ ^{212}Po ($Q_\alpha = 8.95$ MeV, $T_{1/2} = 0.3$ μs) $\rightarrow$ ^{208}Pb, would result in a single event with the total energy up to 4.5 MeV. To suppress such a background, a method of pulse-shape analysis (PSA) of $CdWO_4$ scintillation signals, based on the optimal digital filter [34], was developed [32] and a clear discrimination between γ rays (electrons) and α particles was achieved [32,15,33].

The pulse shape of cadmium tungstate scintillation signal can be described as: $f(t) = \Sigma A_i/(\tau_i - \tau_0)(e^{-t/\tau_i} - e^{-t/\tau_0})$, where A_i are amplitudes and τ_i are decay constants for different light emission components, and τ_0 is the integration constant of electronics ($\approx$0.18 μs). To provide an analytic description of the α or γ signals, the pulse shape resulting from the average of a large number of individual events has been fitted with the sum of three (for α particles) or two (for γ-s) exponential functions, providing the reference pulse shapes $\overline{f}_\alpha(t)$ and $\overline{f}_\gamma(t)$. Comparing two independent calibration measurements with the enriched $^{116}CdWO_4$ crystals (used in the experiment) the following values for the parameters of γ and α pulse shape were obtained: $A_1^\alpha = 80.9(1.9)\%$, $\tau_1^\alpha = 12.7(0.6)$ μs, and $A_2^\alpha = 13.4(1.3)\%$, $\tau_2^\alpha = 3.3(1.1)$ μs, $A_3^\alpha = 5.7(1.0)\%$, $\tau_3^\alpha = 0.96(0.08)$ μs for $\approx$5-MeV α particles, and $A_1^\gamma = 94.3(0.3)\%$, $\tau_1^\gamma = 13.6(0.2)$ μs and $A_2^\gamma = 5.7(0.2)\%$, $\tau_2^\gamma = 2.1(0.1)$ μs for $\approx$1-MeV γ quanta.

In data processing the digital filter was applied to each experimental signal $f(t)$ with the aim to obtain the numerical characteristic of its shape (shape indicator, SI) defined as $\mathrm{SI} = \Sigma f(t_k)P(t_k)/\Sigma f(t_k)$, where the sum is over time channels k, starting from the onset of signal and up to 75 μs, $f(t_k)$ is the digitized amplitude (at the time t_k) of a given signal. The weight function $P(t)$ is defined as $P(t) = \{\overline{f}_\alpha(t) - \overline{f}_\gamma(t)\}/\{\overline{f}_\alpha(t) + \overline{f}_\gamma(t)\}$.

The SI distributions measured with different α and γ sources (some examples are shown in Fig. 1) are well described by Gaussian functions, whose standard deviations $\sigma(\mathrm{SI}_\alpha)$ and $\sigma(\mathrm{SI}_\gamma)$ depend on energy [32,33]. As it is seen from Fig. 1, electrons (γ rays) and α particles are clearly distinguished for the energies above 0.8 MeV ($E_\alpha \approx 3.8$ MeV). Although the pulse-shape discrimination ability worsens at lower energies, even 2-MeV α particles ($E_\alpha^\gamma \approx 0.3$ MeV) can be separated from γ background with reasonable accuracy [33]. An illustration of the PSA of the background events (for energy above 350 keV) is presented in Fig. 2 as three-dimensional distribution of the background events versus the energy and shape indicator. In this plot, one can see two clearly separated populations: the α events, which belong to U/Th families, and $\gamma(\beta)$ events.

In conclusion, the PSA allows us to reject α decays and other background events such as double pulses, the plastic light guide signal overlapping, noise, etc. For example, the α peak of ^{212}Po (the daughter of the ^{212}Bi) was reconstructed with the help of the front edge analysis of the scintillation signals. The energy and time distributions of the sequence of β decay of ^{212}Bi and α decay of ^{212}Po, selected from the background, are presented in Figs. 3(a–c), while a typical example of such an event is shown in Fig. 3(d). Similarly, the

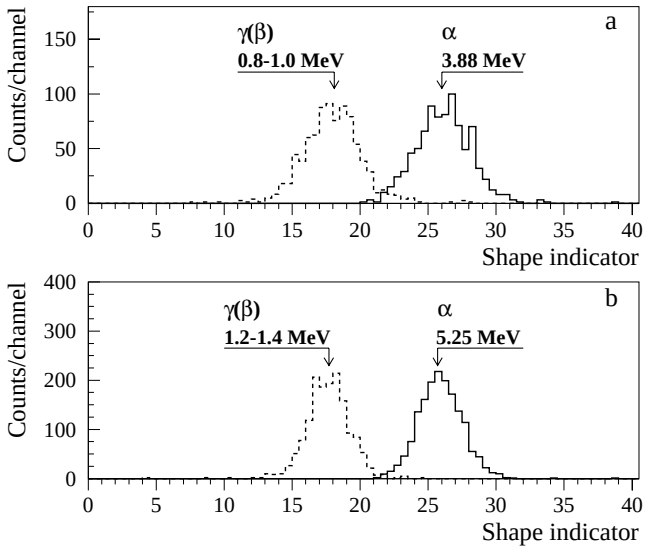

FIG. 1. Examples of the shape indicator distributions for the α particles and γ rays measured by the enriched $^{116}CdWO_4$ crystal scintillator (32×19 mm): (a) E_γ=0.8–1.0 MeV, E_α=3.88 MeV; (b) E_γ=1.2–1.4 MeV, E_α=5.25 MeV. The crystal was irradiated by α particles in a direction perpendicular to the (010) crystal plane [33].

events from the $^{214}Bi\rightarrow^{214}Po\rightarrow^{210}Pb$ chain were recognized, too. As a result, the events caused by two fast decays in both chains ($^{212}Bi\rightarrow^{212}Po\rightarrow^{208}Pb$ and $^{214}Bi\rightarrow^{214}Po\rightarrow^{210}Pb$), which can result in background events with energies up to 4.5 MeV, were discarded from the data.

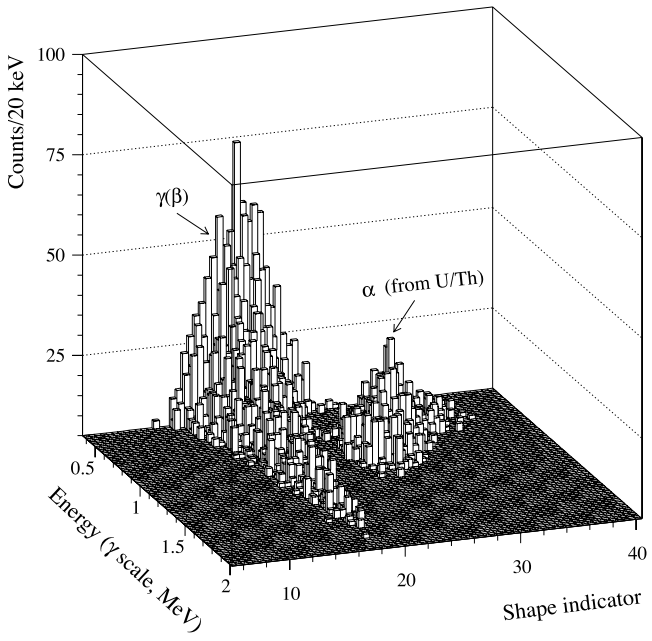

FIG. 2. Three-dimensional distribution of the background events (2975 h of exposition with the $^{116}CdWO_4$ crystals) versus energy and shape indicator. The population of α events belonging to the U/Th families is clearly separated from the population of $\gamma(\beta)$ events.

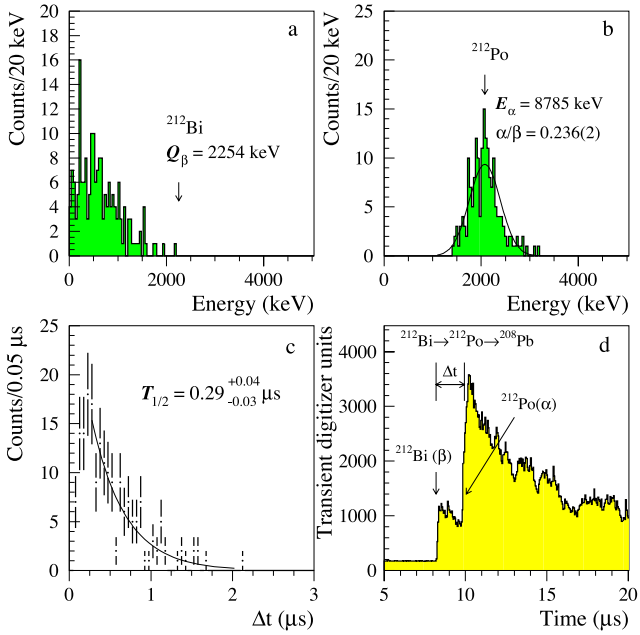

FIG. 3. (Color online) The energy (a,b) and time (c) distributions for the fast sequence of β (^{212}Bi, Q_β=2254 keV) and α [^{212}Po, E_α=8785 keV, $T_{1/2}$=0.299(2) μs] decays selected from the background data by the pulse-shape analysis. (d) Example of such an event in the $^{116}CdWO_4$ scintillator.

C. Time-amplitude analysis of the data

The energy and the arrival time of each event were used for analysis and selection of some decay chains in ^{232}Th, ^{235}U, and ^{238}U families. For instance, the following sequence of α decays from the ^{232}Th family was searched for and observed: ^{224}Ra (Q_α=5.79 MeV)→^{220}Rn (Q_α=6.40 MeV, $T_{1/2}$=55.6 s)→^{216}Po (Q_α=6.91 MeV, $T_{1/2}$=0.145 s)→^{212}Pb. Because the energy of α particles from ^{220}Rn decay corresponds to ≃1.2 MeV in the γ scale of the $^{116}CdWO_4$ detector, the events in the energy region 0.6–2.0 MeV were used as triggers. Then, all events (within 0.6–2.0 MeV) following the triggers in the time interval 10–1000 ms (containing 95% of ^{216}Po decays) were selected. Then in the next step of the analysis, the fast couples found (^{220}Rn and ^{216}Po) were used as triggers to search for preceding α decays of ^{224}Ra. The time window was set as 1–111 s (it contains 74% of ^{220}Rn decays). The obtained α peaks (the α nature of events was confirmed by the pulse-shape analysis described above), as well as the distributions of the time intervals between events are in a good agreement with those expected for α particles of ^{224}Ra, ^{220}Rn, and ^{216}Po (see Fig. 4). On this basis the activity of ^{228}Th in the $^{116}CdWO_4$ crystals was determined as 39(2) μBq/kg. By analyzing the behavior of the ^{228}Th activity within the time interval 5–13 yr after the growth of crystals we have estimated the ^{232}Th activity in the $^{116}CdWO_4$ scintillators as 53(9) μBq/kg, and a limit for the ^{228}Ra activity ⩽4 μBq/kg.

The same technique was applied to the sequence of α decays from the ^{235}U family: ^{223}Ra (Q_α=5.98 MeV) →^{219}Rn (Q_α=6.95 MeV, $T_{1/2}$=3.96 s)→^{215}Po (Q_α=7.53 MeV, $T_{1/2}$=1.78 ms)→^{211}Pb. For the first couple

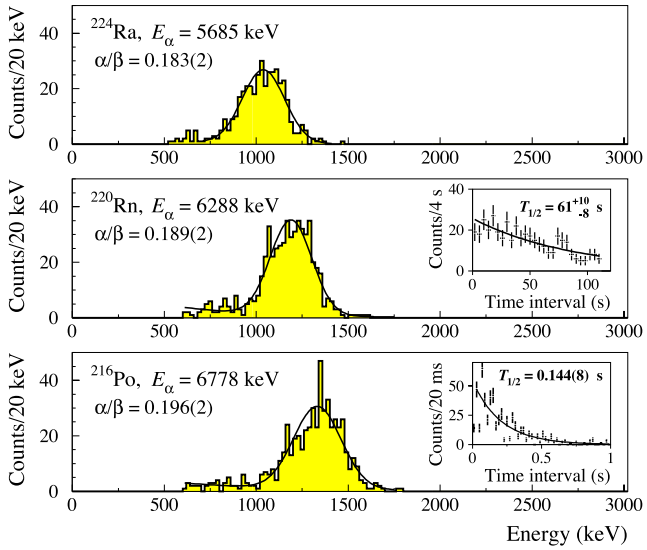

FIG. 4. The α peaks of ^{224}Ra, ^{220}Rn, and ^{216}Po selected by the time-amplitude analysis from the data accumulated during 14 745 h with the $^{116}CdWO_4$ detector. In the insets the time distributions between the first and second (and between second and third) events together with exponential fits are presented. Obtained half-lives of ^{220}Rn and ^{216}Po [61^{+10}_{-8} s and 0.144(8) s, respectively] are in a good agreement with the table values: 55.6(1) s and 0.145(2) s [36].

(^{219}Rn→^{215}Po) all events within 0.6–2.2 MeV were used as triggers, while a time interval 1–10 ms (66% of ^{215}Po decays) and an energy window 0.6–2.2 MeV were set for the second events. The obtained α peaks correspond to an activity of 1.4(9) μBq/kg for the ^{227}Ac impurity in the crystals.

As regards the ^{226}Ra chain (^{238}U family), the following sequence of β and α decays was analyzed: ^{214}Bi (Q_β = 3.27 MeV)→^{214}Po (Q_α = 7.83 MeV, $T_{1/2}$ = 164.3 μs) →^{210}Pb. The obtained results give for the activity of ^{226}Ra in the $^{116}CdWO_4$ crystals a limit $\leqslant 4$ μBq/kg.

Finally, all correlated events found for ^{232}Th, ^{235}U, and ^{238}U families were eliminated from the measured data, while information about measured intrinsic activities of the crystals was used for the background reconstruction in the procedure of data analysis.

III. MEASUREMENTS AND RESULTS

A. Background interpretation

The energy spectrum of the $\gamma(\beta)$ events measured during 13 316 h of the live time in the low background setup with the $^{116}CdWO_4$ crystal scintillators (and selected by the PSA) is shown in Fig. 5. In the low energy region the background is caused mainly by the fourth-forbidden β decay of ^{113}Cd ($T_{1/2}$ = 7.7×10^{15} yr [35], Q_β = 316 keV [36]) and β decay of ^{113m}Cd ($T_{1/2}$ = 14.1 yr, Q_β = 580 keV [36]).[1] The distribution above ≈0.5 MeV is described by the $2\nu2\beta$ decay spectrum of ^{116}Cd with $T^{2\nu}_{1/2}$ = 2.9×10^{19} yr (see below), trace contamination of the enriched and shield crystals by ^{137}Cs and ^{40}K, and external γ rays. The energy distributions for the above mentioned background components were simulated with the help of the code GEANT3.21 [37] and the event generator DECAY4 [38].[2] The least squares fit (χ^2/ndf = 119/108 = 1.1) of the experimental spectrum in the 0.34–2.7 MeV energy interval by the sum of the components listed above (to describe external γ-s an exponential function was used in addition to the ^{40}K, ^{232}Th, and ^{238}U contamination of the PMTs, whose activities were previously measured [27]) gives the following intrinsic activities of the $^{116}CdWO_4$ crystals (in mBq/kg): 1.1(1) for ^{113m}Cd, 0.43(6) for ^{137}Cs, and 0.3(1) for ^{40}K. The ^{40}K contamination of the shielding $CdWO_4$ crystals was calculated to be 1.5(3) mBq/kg. The fitting curve and main components of the background are presented in Fig. 5.

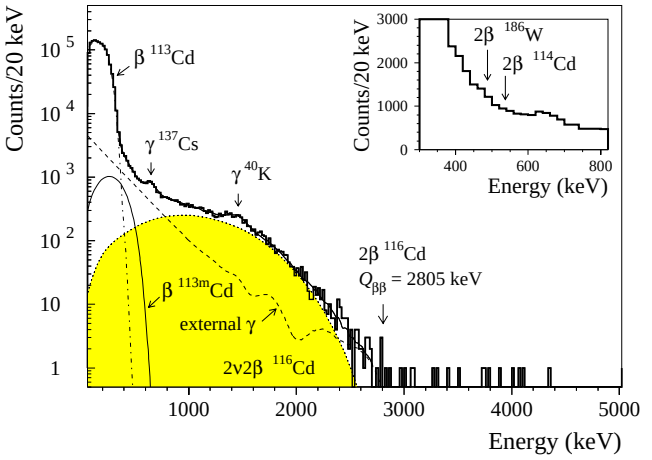

FIG. 5. (Color online) Spectrum of $\gamma(\beta)$ events measured with $^{116}CdWO_4$ detectors during 13 316 h and selected by the pulse-shape analysis. Solid line represents the fit of the data by the background model in the 340–2700-keV-energy interval. Also shown are the most important components of the background: β spectra of ^{113}Cd and ^{113m}Cd, $2\nu2\beta$ spectrum of ^{116}Cd with $T^{2\nu}_{1/2}$=2.9×10^{19} yr, and model distribution of external γ-s.

In addition, the fit was repeated with the described model, into which other impurities were included: ^{210}Pb, ^{234m}Pa (^{238}U family), ^{228}Ac (^{232}Th), and ^{90}Sr (in equilibrium with

[1]The abundance of ^{113}Cd in the enriched crystals was measured with the help of mass spectrometer as δ = 2.15(20)% [25]. The possible presence of ^{113m}Cd in the $CdWO_4$ scintillators was confirmed by the low background measurements with two crystals, where the β spectrum of ^{113m}Cd was observed [30].

[2]The accuracy of the Monte Carlo simulation was checked in the series of the dedicated measurements with the calibration radioactive sources (γ–^{22}Na, ^{54}Mn, ^{60}Co, ^{137}Cs, ^{207}Bi, ^{232}Th; β–^{90}Sr, ^{210}Bi), and with several cadmium tungstate crystals of different sizes. The various detector assemblies were used, beginning from a simplest "detector plus source" design, and ending with the actual low background setup, which includes the anticoincidence scintillators. The measured spectra were simulated with the help of GEANT3.21 and DECAY4 codes as described above. A good agreement between the simulated and experimental results was obtained for each detector configuration, which allows us to use the Monte Carlo simulation for the background reconstruction, and to build up models of the different 2β processes searched for [39].

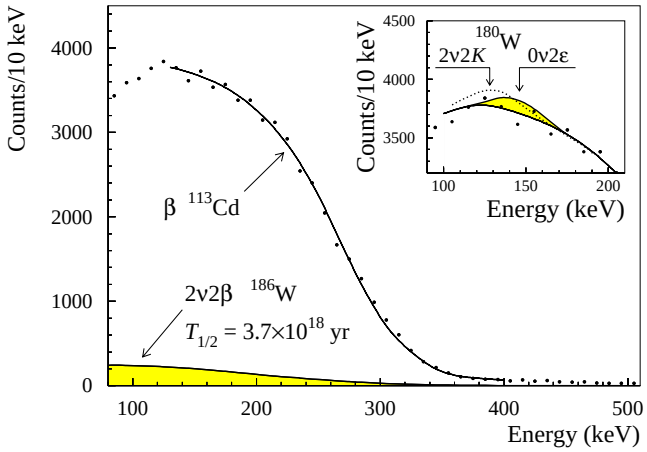

FIG. 6. (Color online) Low energy part of the spectrum measured during 692 h by the $^{116}CdWO_4$ detectors with an energy threshold of 80 keV [the $\gamma(\beta)$ events were selected by the PSA with efficiency of 98%]. The fitting curve is drawn by the solid line. Shadowed distribution is $2\nu2\beta$ decay spectrum of ^{186}W with $T^{2\nu}_{1/2} = 3.7\times10^{18}$ yr excluded at 90% C.L. Inset: The part of the spectrum together with the $2\nu2K$ peak of ^{180}W with $T^{2\nu2K}_{1/2} = 0.7 \times 1\ 0^{17}$ yr (dotted line) and $0\nu2\varepsilon$ peak of ^{180}W with $T^{0\nu2\varepsilon}_{1/2} = 0.9 \times10^{17}$ yr (shadowed), both excluded at 90% C.L.

^{90}Y). However, only limits on their activities in the $^{116}CdWO_4$ scintillators were obtained, as follows (mBq/kg): ^{210}Pb$\leqslant$0.4, ^{234m}Pa$\leqslant$0.2, ^{228}Ac (^{228}Ra) $\leqslant$0.1, and ^{90}Sr $\leqslant$0.2.

The lowest energy part of the experimental spectrum is dominated by the β spectrum of ^{113}Cd (see Fig. 6). To determine its activity, the background of the $^{116}CdWO_4$ detectors was measured during 692 h with the energy threshold of 80 keV, which allows us to extend the PSA technique to this energy region. Fitting the data by a sum of the simulated β spectrum of ^{113}Cd and an exponential function (to describe residual background) we estimate the activity of ^{113}Cd in the enriched crystals as 91(5) mBq/kg. It corresponds to an abundance of this isotope in the $^{116}CdWO_4$ crystals $\delta = 1.9(2)\%$, which is in agreement with the result of mass-spectrometric measurement $\delta = 2.15(20)\%$ [25].

All data on radioactive contamination of the $^{116}CdWO_4$ crystal scintillators are summarized in Table I.

B. Two-neutrino double β decay of ^{116}Cd

The level scheme of the ^{116}Cd-^{116}In-^{116}Sn triplet [36] is depicted in Fig. 7(a), while the response functions of the $^{116}CdWO_4$ detector for the different channels of the $2\nu2\beta$ and $0\nu2\beta$ decay of ^{116}Cd (simulated with the help of GEANT3.21 and DECAY4 codes) are shown in Figs. 7(b) (g.s. $\rightarrow$g.s. transitions, where g.s. corresponds to ground state) and 8 (transitions to excited levels of ^{116}Sn).

Earlier, after 4629 h of data accumulation in our experiment, the preliminary half-life value of two-neutrino 2β decay of ^{116}Cd was reported as $T^{2\nu}_{1/2} = 2.6 \pm 0.1(\text{stat})^{+0.7}_{-0.4}(\text{syst}) \times 10^{19}$ yr [15]. In the present work, with the aim to derive a refined $T^{2\nu}_{1/2}$ value, we are using the advantage of higher statistics (12 649 h) collected after the last upgrade of the setup

TABLE I. Activities of different nuclides present in the $^{116}CdWO_4$ crystal scintillators.

Chain	Nuclide	Activity (mBq/kg)
^{232}Th	^{232}Th	0.053(9)
	^{228}Ra	$\leqslant$0.004
	^{228}Th	0.039(2)
^{238}U	^{238}U+^{234}U	$\leqslant$0.6
	^{234m}Pa	$\leqslant$0.2
	^{230}Th	$\leqslant$0.5
	^{226}Ra	$\leqslant$0.004
	^{210}Pb	$\leqslant$0.4
^{235}U	^{227}Ac	0.0014(9)
	^{40}K	0.3(1)
	^{90}Sr	$\leqslant$0.2
	^{113}Cd	91(5)
	^{113m}Cd	1.1(1)
	^{137}Cs	0.43(6)

in 1999 when spectrometric parameters of the detector (in particular, the energy resolution and pulse shape discrimination ability) were improved. The $^{116}CdWO_4$ crystals contain 4.54×10^{23} nuclei of ^{116}Cd, therefore the exposure of the experiment is 6.56×10^{23} nuclei$\times$yr. The total efficiency for detecting the $2\nu2\beta$ decay of ^{116}Cd by the $^{116}CdWO_4$ crys-

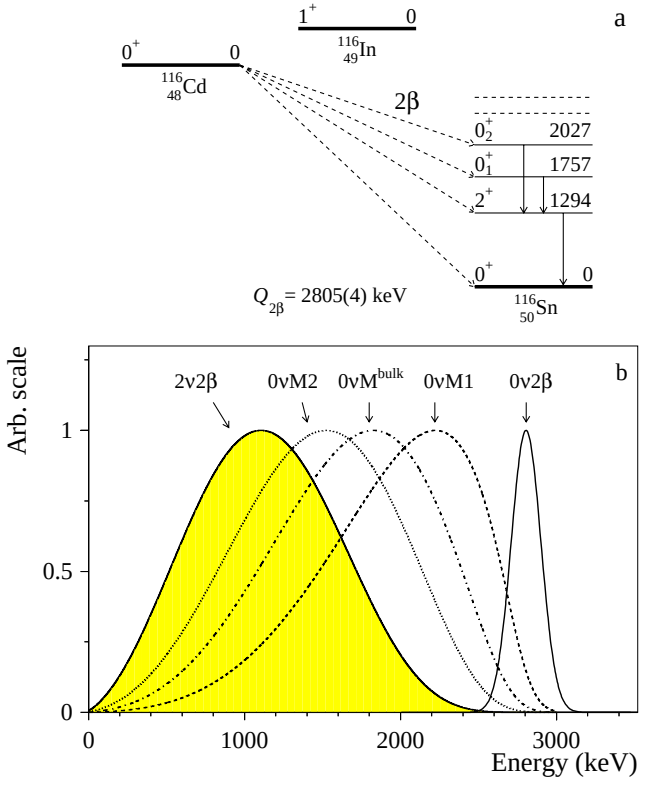

FIG. 7. (a) (Color online) The level scheme of the ^{116}Cd-^{116}In-^{116}Sn triplet. The $Q_{\beta\beta}$ energy is taken from [40]. (b) Simulated response functions of the $^{116}CdWO_4$ crystal scintillators for the 2ν and 0ν modes of the 2β decay of ^{116}Cd to the ground level of ^{116}Sn.

TABLE II. Different origins of the systematical uncertainties and their contributions to the half-life value of ^{116}Cd two-neutrino 2β decay.

Origin of the systematic error	Range	Contribution to $T^{2\nu}_{1/2}$ value, 10^{19} yr
Live measuring time	$(96\pm2)\%$	±0.06
Efficiency of the PS analysis	97^{+1}_{-3} %	$+0.03,-0.09$
Detection efficiency of the $2\nu2\beta$ decay (GEANT model uncertainty)	$(96\pm3)\%$	±0.09
Fit in different energy regions		$+0.2,-0.3$
^{90}Sr–^{90}Y and ^{234m}Pa impurity in $^{116}CdWO_4$	$\leqslant0.3$ mBq/kg	$+0.35$

tals is calculated as 0.93 (Monte Carlo simulation gives the registration efficiency of the $2\nu2\beta$ decay events as $\eta_{mc}=0.96$, while the efficiency of the PSA selection of $\gamma(\beta)$ events is $\eta_{psa}=0.97$).

The part of the experimental spectrum used for the data analysis is depicted in Fig. 9. The data in the energy interval 800–2800 keV were simulated with the help of the GEANT3.21 package and the event generator DECAY4. In addition to the ^{116}Cd two-neutrino 2β decay distribution, only three background components were considered. These are ^{40}K contamination of the enriched and nonenriched $CdWO_4$ scintillators, and external γ background caused by ^{40}K, ^{232}Th, and ^{238}U contamination of the PMTs. The radioactive impurities of each PMT were previously measured as (2–4) Bq/PMT for ^{40}K, and (0.4–2.2) and (0.1–0.2) Bq/PMT for ^{226}Ra and ^{228}Th activity, respectively [27].

The fit of experimental data in the energy interval 860–2700 keV (χ^2/ndf$=64/86=0.7$) gives the following results: the activities of ^{40}K inside the enriched and nonenriched $CdWO_4$ crystals are equal to 0.4(2) and 1.6(4) mBq/kg, respectively; the half-life value of the $2\nu2\beta$ decay of ^{116}Cd is $2.93\pm0.06(\text{stat})\times10^{19}$ yr (the corresponding activity in the enriched crystals is about 1 mBq/kg).[3]

The quality of our results can be judged on the basis of the deduced $2\nu2\beta$ Kurie plot: $K(\varepsilon)=[S(\varepsilon)/\{(\varepsilon^4+10\varepsilon^3+40\varepsilon^2+60\varepsilon+30)\varepsilon\}]^{1/5}$, where S is the number of events with energy ε (in units of electron mass) in the experimental spectrum after background subtraction. For the true $2\nu2\beta$ decay distribution, such a Kurie plot should be a straight line $K(\varepsilon)\sim(Q_{2\beta}-\varepsilon)$. The obtained experimental Kurie plot is depicted in the inset of Fig. 9, from which one can see that in the energy region 0.9–2.5 MeV it is indeed well fitted by the straight line with $Q_{2\beta}=2808(43)$ keV (the table value is $Q_{2\beta}=2805(4)$ keV [40]).[4]

It should be stressed that statistics collected in our experiment (9846 events of $2\nu2\beta$ decay of ^{116}Cd within the energy interval 800–2800 keV) and a signal to background ratio (3:1 for the energy interval 1.2–2.8 MeV and 8:1 for the energy range 1.9–2.2 MeV) are among the highest ones reached up to date in 2β decay experiments [6–8].

Different origins of systematical uncertainties of the measured half-life were taken into account (see Table II). The main ones are the above mentioned half-life changes for the fitting in different energy regions, and possible traces of the β active nuclides ^{234m}Pa and ^{90}Y (daughter of ^{90}Sr) in the $^{116}CdWO_4$ crystals. In fact, both these causes are related to background model description which is a typical problem of data interpretation in low background experiments. From the upper limit on ^{226}Ra contamination, derived with the help of the time-amplitude analysis of the data, it is obtained that activity of ^{238}U (and therefore of ^{234m}Pa) in the enriched crystals is less than 0.7 mBq/kg.[5] To estimate a systematic uncertainty, both β nuclides (^{234m}Pa and ^{90}Sr–^{90}Y) were included in the fitting procedure, which leads to the stronger bound on their total activity $\leqslant0.3$ mBq/kg.

The final half-life value is equal to

$$T^{2\nu}_{1/2}=2.9\pm0.06(\text{stat})^{+0.4}_{-0.3}(\text{syst})\times10^{19}\ \text{yr}.$$

This value is in agreement with our preliminary result $T^{2\nu}_{1/2}=2.6^{+0.7}_{-0.4}\times10^{19}$ yr [15], and with those measured earlier in other experiments: $T^{2\nu}_{1/2}=2.6^{+0.9}_{-0.5}\times10^{19}$ yr [41], $T^{2\nu}_{1/2}=2.7^{+0.5}_{-0.4}(\text{stat})^{+0.9}_{-0.6}(\text{syst})\times10^{19}$ yr [24], and $T^{2\nu}_{1/2}=3.75\pm0.35(\text{stat})\pm0.21(\text{syst})\times10^{19}$ yr [42].

[3]The fitting interval has been chosen as a compromise between several contradicting demands: (i) the high statistics accumulated; (ii) the large ratio of the effect to background; (iii) the maximal energy range of the $2\nu2\beta$ decay spectrum; (iv) the goodness of the fit; (v) the reasonably small uncertainties of fitting parameters, etc. It is remarkable to note that the results of the fit were rather stable for the different energy intervals in the range (800–2800) keV; so, the corresponding values of half-life varied in the range of $(2.6–3.1)\times10^{19}$ yr. Actually, such changes of the half-life value result mainly from the background model uncertainties.

[4]To take into account the energy resolution of the detector, the fitting procedure was repeated by using the convolution of the theoretical $2\nu2\beta$ distribution $\rho(\varepsilon)=A\varepsilon(\varepsilon^4+10\varepsilon^3+40\varepsilon^2+60\varepsilon+30)(Q_{2\beta}-\varepsilon)^5$ with the detector resolution function (A, which is inverse proportional to $T^{2\nu}_{1/2}$, and $Q_{2\beta}$ were taken as free parameters). The fit in the energy region 1.2–2.8 MeV yields similar $Q_{2\beta}$ and half-life values: $Q_{2\beta}=2748(42)$ keV; $T_{1/2}=2.9(1)\times10^{19}$ yr.

[5]This estimation was derived from the limit on the ^{226}Ra activity ($\leqslant4$ μBq/kg), conservatively supposing that all ^{226}Ra nuclei were produced from ^{238}U contamination in the crystals during ≈13 yr after their growth. An analysis of α spectra [33] gives estimation of $\leqslant0.6$ mBq/kg for the total activity of ^{238}U and ^{234}U.

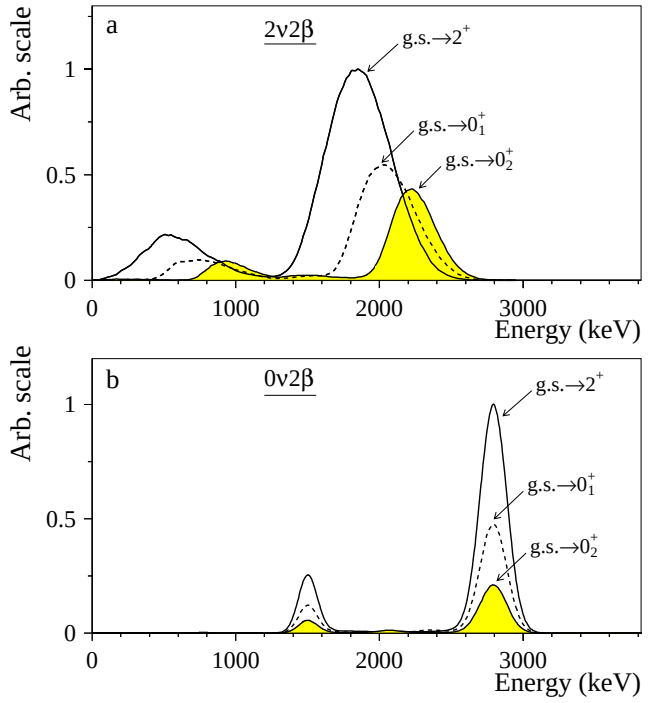

FIG. 8. (Color online) Simulated response functions of the $^{116}CdWO_4$ crystal scintillators for the $2\nu2\beta$ (a) and $0\nu2\beta$ (b) decay of ^{116}Cd to excited levels of ^{116}Sn.

Besides, we have also searched for the possible $2\nu2\beta$ decay of ^{116}Cd to excited levels of ^{116}Sn [see Fig. 8(a)]: 2^+ with $E_{lev}=1294$ keV, 0_1^+ with $E_{lev}=1757$ keV, and 0_2^+ with $E_{lev}=2027$ keV. However, the probabilities of such 2β transitions should be strongly suppressed due to reduced energy releases (for example, the theoretical predictions for their half-lives are in the range of 10^{22}–10^{24} yr [8]). Because of the absence in the experimental data of any indications on these processes, we only set the bounds on their half-lives with the help of the formula: $\lim T_{1/2}=\ln 2 N t\eta/\lim S$, where N is the number of ^{116}Cd nuclei, t the measuring time, η the total detection efficiency, and $\lim S$ the number of events of the effect searched for, which can be excluded with a given confidence level. The value of the detection efficiency was calculated by using the GEANT3.21 and DECAY4 codes as $\eta_{mc}(2^+)=0.18$, $\eta_{mc}(0_1^+)=0.09$, and $\eta_{mc}(0_2^+)=0.06$. Taking into account the efficiency of the pulse-shape analysis $\eta_{psa}=0.97$, this gives the total efficiencies $\eta(2^+)=0.18$, $\eta(0_1^+)=0.09$, and $\eta(0_2^+)=0.06$. To estimate the value of $\lim S$, the fit described above was repeated in the energy interval 1.7–2.7 MeV by adding the simulated response functions for the effect searched for. It yields $S=-33\pm108$ counts (2^+), $S=-53\pm59$ counts (0_1^+), and $S=-3\pm47$ counts (0_2^+), which corresponds, in accordance with the Feldman-Cousins procedure [43] recommended by the Particle Data Group [44], to the restrictions on the half-lives of $2\nu2\beta$ decay of ^{116}Cd to excited levels of $2\nu2\beta$ decay of ^{116}Cd to excited levels of ^{116}Sn at 90% (68%) C.L.:

$$T_{1/2}^{2\nu}(\text{g.s.}\rightarrow 2^+)\geqslant 0.6(1.1)\times 10^{21}\ \text{yr},$$

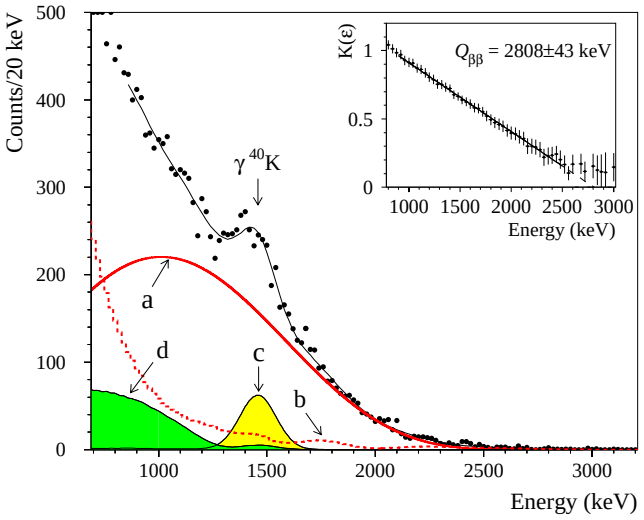

FIG. 9. (Color online) The part of $\gamma(\beta)$ spectrum measured with $^{116}CdWO_4$ detectors during 12 649 h, which was used for the determination of the half-life of $2\nu2\beta$ decay of ^{116}Cd. Also shown are the most important model components: (a) the $2\nu2\beta$ spectrum of ^{116}Cd; (b) external γ background caused by ^{40}K, ^{232}Th, and ^{238}U contamination of the PMTs; ^{40}K contamination of the nonenriched (c) and enriched (d) $CdWO_4$ scintillators. Solid line represents the fit of the data in the 860–2700 keV energy interval. Inset: The $2\nu2\beta$ decay Kurie plot and its fit by a straight line in the 900–2500-keV-energy region.

$$T_{1/2}^{2\nu}(\text{g.s.}\rightarrow 0_1^+)\geqslant 0.8(2.2)\times 10^{21}\ \text{yr},$$

$$T_{1/2}^{2\nu}(\text{g.s.}\rightarrow 0_2^+)\geqslant 0.4(0.6)\times 10^{21}\ \text{yr}.$$

C. Neutrinoless double β decay of ^{116}Cd

The part of the spectrum of the $^{116}CdWO_4$ crystals measured during 14 183 h in anticoincidence with the shielding detectors and after the time-amplitude and pulse-shape selection is shown in Fig. 10. The exposure corresponds to 7.41×10^{23} (nuclei of ^{116}Cd)$\times$yr. This spectrum includes also data obtained in the first part of the experiment [15]. The energy resolution and the efficiency of the pulse-shape discrimination were calculated for the full exposition, taking into account results of the calibration measurements. For instance, for the total spectrum the energy resolution at 2.8 MeV was 8.9%.

The background rate in the energy interval 2.5–3.2 MeV is 0.037(10) counts/(yr kg keV). The peak of $0\nu2\beta$ decay is absent, thus we obtain a lower limit on the half-life. The efficiency to detect this peak in crystals was calculated by the Monte Carlo method (with the help of GEANT3.21 and DECAY4 codes) as $\eta_{mc}=0.83$. Again by taking into account the efficiency of the pulse-shape analysis $\eta_{psa}=0.96$, it yields a total efficiency $\eta=0.80$. To estimate $\lim S$, the part of the spectrum in the 2.0–3.6 MeV energy interval was fitted by the sum of the simulated $0\nu2\beta$ peak and three background functions: $2\nu2\beta$ decay (contribution to the experimental spectrum is $\approx$ 83%), γ rays from PMTs ($\approx$14%), and background from the intrinsic chain ^{228}Th ($\approx$3%). For the fit

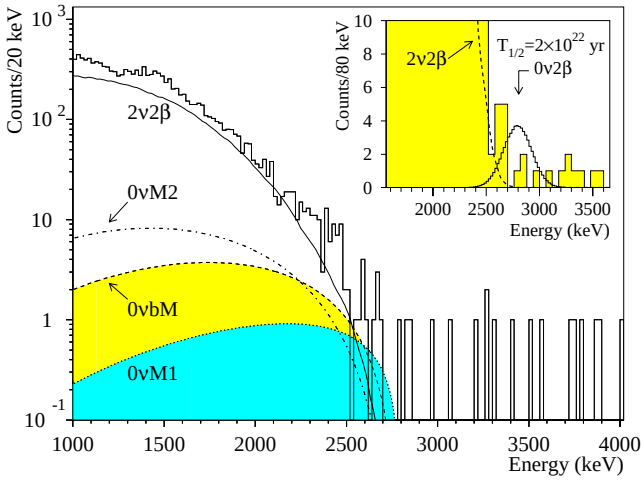

FIG. 10. (Color online) The high energy part of the experimental spectrum of the $^{116}CdWO_4$ detectors measured during 14 183 h (histogram) together with the fit from $2\nu2\beta$ contribution ($T^{2\nu}_{1/2}=2.9\times10^{19}$ yr). The smooth curves $0\nu M1$, $0\nu M2$, and $0\nu bM$ are excluded with 90% C.L. distributions of $0\nu2\beta$ decay of ^{116}Cd with emission of one, two, and bulk Majorons, respectively: $T^{0\nu M1}_{1/2}=8.0\times10^{21}$ yr, $T^{0\nu M2}_{1/2}=8.0\times10^{20}$ yr, and $T^{0\nu bM}_{1/2}=1.7\times10^{21}$ yr. In the inset the expected peak from $0\nu2\beta$ decay with $T^{0\nu}_{1/2}=2\times10^{22}$ yr is shown.

these background activities were taken as free parameters and varied within their errors. This maximum likelihood fit (χ^2/ndf=37/33=1.1) gives the area of the $0\nu2\beta$ peak as $S=0.3\pm1.3$ counts, which corresponds to $\lim S=2.4$ (1.6) counts with 90% (68%) C.L.,[6] and to a half-life limit for the $0\nu2\beta$ decay of ^{116}Cd:

$$T^{0\nu}_{1/2}\geq1.7(2.6)\times10^{23}\ \text{yr at 90\%(68\%)C.L.}$$

Excited levels of ^{116}Sn with $E_{lev}\leq Q_{2\beta}$ can be also populated in the $0\nu2\beta$ decay of ^{116}Cd [the corresponding response functions are shown in Fig. 8(b)]. The full absorption of all emitted particles should result in a peak with $E=Q_{2\beta}$. The full peak efficiencies calculated with the help of the GEANT3.21 and DECAY4 codes for the $0\nu2\beta$ decay to the first, second, and third excited levels of ^{116}Sn are $\eta_{mc}(2^+)=0.14$, $\eta_{mc}(0^+_1)=0.07$, and $\eta_{mc}(0^+_2)=0.03$. These numbers result in the following restrictions on half-life of ^{116}Cd $0\nu2\beta$ decay to excited levels of ^{116}Sn at 90% (68%) C.L.:

$$T^{0\nu}_{1/2}(\text{g.s.}\rightarrow2^+)\geq2.9(4.3)\times10^{22}\ \text{yr},$$

$$T^{0\nu}_{1/2}(\text{g.s.}\rightarrow0^+_1)\geq1.4(2.2)\times10^{22}\ \text{yr},$$

$$T^{0\nu}_{1/2}(\text{g.s.}\rightarrow0^+_2)\geq0.6(0.9)\times10^{22}\ \text{yr}.$$

To obtain the half-life limits for the $0\nu2\beta$ decay with emission of one, two, and bulk [45] Majoron(s), the measured spectrum was fitted in the energy region 1.6–2.8 MeV by using the same model of background as for the $0\nu2\beta$ decay fitting procedure. As a result, the number of events under a theoretical 0νM1 curve was determined as -37 ± 56, giving no statistical evidence for the effect. Again, following the Particle Data Group (PDG) recommendation, it leads to an upper limit of 59 (25) events at 90% (68%) C.L., which together with an efficiency value $\eta_{mc}=0.905$ corresponds to a half-life limit

$$T^{0\nu M1}_{1/2}\geq0.8(1.8)\times10^{22}\ \text{yr at 90\%(68\%)C.L.}$$

A similar procedure for the $0\nu2\beta$ decay with two and bulk Majorons emission gives the following results at 90% (68%) C.L.:

$$T^{0\nu M2}_{1/2}\geq0.8(1.4)\times10^{21}\ \text{yr},$$

$$T^{0\nu bM}_{1/2}\geq1.7(2.3)\times10^{21}\ \text{yr}.$$

Excluded with 90% C.L. distributions of $0\nu M1$,$0\nu M2$, and 0ν decay with bulk Majoron emission are shown in Fig. 10.

D. Limits on 2β decay processes in ^{106}Cd, ^{108}Cd, ^{114}Cd, ^{180}W, and ^{186}W

The $^{116}CdWO_4$ crystals contain not only ^{116}Cd nuclei but several other potentially 2β decaying isotopes: ^{106}Cd with abundance $\delta=0.16\%$ [25] and $Q_{\beta\beta}=2771$ keV [40], ^{108}Cd ($\delta=0.11\%$ [25], $Q_{\beta\beta}=269$ keV), ^{114}Cd ($\delta=6.5\%$ [25], $Q_{\beta\beta}=537$ keV), ^{180}W ($\delta=0.12\%$ [46], $Q_{\beta\beta}=146$ keV), and ^{186}W ($\delta=28.4\%$ [46], $Q_{\beta\beta}=488$ keV). It allows us to establish bounds on 2β decay processes in these nuclides.

The spectrum of Fig. 5 was used to search for the $0\nu2\beta$ decay of ^{114}Cd (g.s.-g.s. transition) and for the $0\nu2\beta$ decay of ^{186}W to the ground and to the first excited (2^+) levels of ^{186}Os. In the energy range of interest (440–600 keV), where the background rate is equal to 0.295(3) counts/(day keV kg), there is no indication for the positive $0\nu2\beta$ decay peak of ^{186}W searched for. Hence, we can only set a limit on its probability. Taking into account the registration efficiency of the $^{116}CdWO_4$ scintillators for this process ($\eta_{mc}=0.99$), and the efficiency of the PSA ($\eta_{psa}=0.95$), the total detection efficiency is $\eta=0.94$.

The value of $\lim S$ was determined by using the standard χ^2 procedure, where the experimental spectrum in the (380–1200)-keV-energy interval was fitted by the sum of the $0\nu2\beta$ decay peak being sought and the background components determined above (^{113m}Cd, ^{137}Cs, exponential function representing external γ rays, and $2\nu2\beta$ decay of ^{116}Cd). The fit (χ^2/ndf=38/36=1.1) yields the peak area (-21 ± 95)

[6]As it was noted earlier (see Sec. II A), the energy resolution of the spectrometer was carefully tested during the experiment. Nevertheless, to check the possible influence of energy resolution on the lim$S$ estimation, the fit has been repeated for the different FWHM values (8%, 9%, 10%, and 11% at 2.8 MeV), which were taken into account in all the background models. As it was found, the variation of the lim$S$ does not exceed $\pm15\%$. In addition, the fit has been also performed for the different energy intervals in the energy region 1900–3800 keV, and resulting changes of the lim$S$ were within $\pm$ 25% of the central value.

counts, i.e., no evidence for the effect. Using the PDG recommendation, one can get $\lim S = 136$ (75) counts at 90% (68%) C.L. Taking into account these values, the efficiency $\eta = 0.94$, and the number of ^{186}W nuclei (1.56×10^{23}), we derive the following half-life limit on the $0\nu 2\beta$ decay of ^{186}W to the ground level of ^{186}Os:

$$T_{1/2}^{0\nu} \geq 1.1(2.1) \times 10^{21} \text{ yr at } 90\%(68\%)\text{C.L.}$$

In the case of ^{186}W neutrinoless 2β decay to the first excited (2^+) level of ^{186}Os, γ quanta with an energy of 137 keV (deexcitation of the 2^+ level of ^{186}Os) will be emitted. Due to practically full absorption of these γ quanta in the $^{116}CdWO_4$ crystals, the expected response function does not differ from that for transition to ground state. The total efficiency is equal to $\eta = 0.92$, and leads to the half-life limit

$$T_{1/2}^{0\nu}(\text{g.s.} \rightarrow 2^+) \geq 1.1(2.0) \times 10^{21} \text{ yr at } 90\%(68\%)\text{C.L.}$$

For the $0\nu 2\beta$ decay of ^{186}W with an emission of Majoron, the fit of the spectrum gives

$$T_{1/2}^{0\nu M1} \geq 1.2(1.4) \times 10^{20} \text{ yr at } 90\%(68\%)\text{C.L.}$$

To estimate the lower limit for the $2\nu 2\beta$ decay of ^{186}W, we have considered the background spectrum accumulated during 692 h with the low energy threshold (Fig. 6). Because practically 100% of the β particles from the expected $2\nu 2\beta$ decay are absorbed in the crystals, the total efficiency is determined by the PSA ($\eta = \eta_{psa} = 0.98$). A simple model (which includes the $2\nu 2\beta$ spectrum of ^{186}W, the β spectrum of ^{113}Cd, and an exponential function) was used to describe the experimental data in the energy interval 130–450 keV. The fit ($\chi^2/\text{ndf} = 42/29 = 1.5$) gives 489 ± 1119 events for the effect searched for. It yields 2324 (1608) counts excluded at 90% (68%) C.L., and the half-life limit for the $2\nu 2\beta$ decay of ^{186}W:

$$T_{1/2}^{2\nu} \geq 3.7(5.3) \times 10^{18} \text{ yr at } 90\%(68\%)\text{C.L.}$$

The $2\nu 2\beta$ decay distribution of ^{186}W excluded at 90% C.L. is depicted in Fig. 6.

The same method gives the bound for $2\nu 2\beta$ transition to the first (2^+) excited level of ^{186}Os:

$$T_{1/2}^{2\nu}(\text{g.s.} \rightarrow 2^+) \geq 1.0(1.3) \times 10^{19} \text{ yr at } 90\%(68\%)\text{C.L.}$$

Similar procedures were used to search for 2β decay processes in ^{114}Cd and the obtained bounds are presented in Table III.

In accordance with the level scheme of the ^{180}W–^{180}Ta–^{180}Hf triplet [36], the double electron capture (2ε) of ^{180}W ($Q_{2\varepsilon} = 146$ keV) is allowed. In the case of 2ν double electron capture from the K shell ($2\nu 2K$), the total energy released in a detector is equal to $2E_K$ (where $E_K = 65.4$ keV is the binding energy of electrons on the K shell of hafnium atom), while the rest of the energy ($Q_{2\varepsilon} - 2E_K \approx 15$ keV) is carried away by neutrinos. For the neutrinoless double electron capture ($0\nu 2\varepsilon$), all available energy (transferred to X rays, Auger electrons, γ quanta, or conversion electrons) will result in a peak at $Q_{2\varepsilon} = 146$ keV value.

To set the limits on the $0\nu 2\varepsilon$ process in ^{180}W, the background spectrum measured with the $^{116}CdWO_4$ detector during 692 h (Fig. 6) was fitted in the 90–240-keV energy interval, which gives 91 ± 177 counts for the peak searched for ($\chi^2/\text{ndf} = 18/14 = 1.3$). These numbers lead to an upper limit of 381 (268) counts at 90% (68%) C.L. Taking into account the total efficiency $\eta = \eta_{psa} = 0.98$ and the number of ^{180}W nuclei (6.57×10^{20}), one can calculate the half-life limit

$$T_{1/2}^{0\nu 2\varepsilon} \geq 0.9\ (1.3) \times 10^{17} \text{ yr at } 90\%(68\%)\text{C.L.}$$

The same method gives restriction for the $2\nu 2K$ process in ^{180}W:

$$T_{1/2}^{2\nu 2K} \geq 0.7(0.8) \times 10^{17} \text{ yr at } 90\%(68\%)\text{C.L.}$$

The peaks of the $0\nu 2\varepsilon$ and $2\nu 2K$ captures in ^{180}W excluded at 90% C.L. are shown in the inset of Fig. 6.

Similarly, by using the described procedures, the bounds on neutrinoless double electron capture in ^{108}Cd were extracted from our experimental data. Because of absence of the peak at the transition energy ($Q_{\beta\beta} = 269$ keV), the fit of the spectrum of Fig. 6 yields the half-life limit for the $0\nu 2\varepsilon$ capture in ^{108}Cd: $T_{1/2}^{0\nu 2\varepsilon} \geq 1.5(2.5) \times 10^{17}$ yr at 90% (68%) C.L.

To search for the $2\nu 2K$ capture in ^{106}Cd and ^{108}Cd with an energy release $2E_K \approx 49$ keV (where $E_K = 24.4$ keV is the binding energy of electrons on the K shell of palladium atom), a detector with a low energy threshold is needed. With this aim the results of dedicated measurements (433 h) with the nonenriched $CdWO_4$ crystal (454 g) were used [35]. The energy resolution of this detector at 60 keV (γ rays of ^{241}Am) was FWHM = 25 keV, while the energy threshold was ≈ 40 keV. This crystal contains 9.5×10^{21} and 6.8×10^{21} nuclei of ^{106}Cd and ^{108}Cd, respectively. The measured spectrum [35] was fitted by the sum of the expected peak at the energy of 49 keV and a background model (β spectrum of ^{113}Cd). It gives the following half-life limits on $2\nu 2\varepsilon$ capture: $T_{1/2}^{2\nu 2K} \geq 5.8\ (9.5) \times 10^{17}$ yr at 90% (68%) C.L. for ^{106}Cd, and $T_{1/2}^{2\nu 2K} \geq 4.1\ (6.7) \times 10^{17}$ yr at 90% (68%) C.L. for ^{108}Cd.

As it is visible from the level scheme of the ^{106}Cd-^{106}Ag-^{106}Pd triplet [Fig. 11(a)], besides the double electron capture (2ε) also the double positron decay ($\beta^+\beta^+$), and the electron capture and positron decay ($\varepsilon\beta^+$) are allowed for ^{106}Cd (both to the ground state and to excited levels of ^{106}Pd). The Monte Carlo simulated response functions of the $^{116}CdWO_4$ detector to the 0ν modes of these processes are presented in Fig. 11(b). One can see from this figure that each of the mentioned processes will result in the full absorption peak at the energy 2771 keV with the width FWHM = 216 keV. The values of the efficiency to detect such a peak were calculated as follows: η_{mc} ($0\nu 2\varepsilon$, g.s. $\rightarrow$g.s.) = 0.015; η_{mc} ($0\nu\varepsilon\beta^+$, g.s.$\rightarrow$g.s.) = 0.128; η_{mc} ($0\nu\varepsilon\beta^+$, g.s.$\rightarrow 2^+$, 512 keV)=0.059; η_{mc} ($0\nu\beta^+\beta^+$, g.s. $\rightarrow$g.s.)=0.027; η_{mc} ($0\nu\beta^+\beta^+$, g.s.$\rightarrow 2^+$, 512 keV)

TABLE III. Total list of the results obtained on the 2β decay processes in Cd and W nuclides.

Nuclide	Decay mode	Transition	(level energy)	$T_{1/2}$ limit or value (yr) 90% (68)% C.L.
^{106}Cd	2ε	0ν	g.s.-g.s.	$\geqslant 0.8(1.7)\times 10^{19}$
	$\varepsilon\beta^+$	0ν	g.s.-g.s.	$\geqslant 0.7(1.6)\times 10^{20}$
		0ν	g.s.-2_1^+ (511.9 keV)	$\geqslant 3.1(7.2)\times 10^{19}$
		0ν	g.s.-2_2^+ (1128.0 keV)	$\geqslant 1.4(3.3)\times 10^{19}$
		0ν	g.s.-0_1^+ (1133.8 keV)	$\geqslant 1.4(3.2)\times 10^{19}$
	$2\beta^+$	0ν	g.s.-g.s.	$\geqslant 1.4(3.3)\times 10^{19}$
		0ν	g.s.-2_1^+ (511.9 keV)	$\geqslant 0.6(1.5)\times 10^{19}$
	$2K$	2ν	g.s.-g.s.	$\geqslant 5.8(9.5)\times 10^{17}$
	$\varepsilon\beta^+$	2ν	g.s.-g.s.	$\geqslant 1.2(2.0)\times 10^{18}$
	$2\beta^+$	2ν	g.s.-g.s.	$\geqslant 5.0(8.2)\times 10^{18}$
^{108}Cd	2ε	0ν	g.s.-g.s.	$\geqslant 1.5(2.5)\times 10^{17}$
	$2K$	2ν	g.s.-g.s.	$\geqslant 4.1(6.7)\times 10^{17}$
^{114}Cd	$2\beta^-$	0ν	g.s.-g.s.	$\geqslant 2.5(4.1)\times 10^{20}$
	$2\beta^-$	2ν	g.s.-g.s.	$\geqslant 6.0(9.3)\times 10^{17}$
^{116}Cd	$2\beta^-$	0ν	g.s.-g.s.	$\geqslant 1.7(2.6)\times 10^{23}$
		0ν	g.s.-2^+ (1293.5 keV)	$\geqslant 2.9(4.3)\times 10^{22}$
		0ν	g.s.-0_1^+ (1756.8 keV)	$\geqslant 1.4(2.2)\times 10^{22}$
		0ν	g.s.-0_2^+ (2027.3 keV)	$\geqslant 0.6(0.9)\times 10^{22}$
		$0\nu M1$	g.s.-g.s.	$\geqslant 0.8(1.8)\times 10^{22}$
		$0\nu M2$	g.s.-g.s.	$\geqslant 0.8(1.4)\times 10^{21}$
		$0\nu bM$	g.s.-g.s.	$\geqslant 1.7(2.3)\times 10^{21}$
	$2\beta^-$	2ν	g.s.-g.s.	$=2.9^{+0.4}_{-0.3}\times 10^{19}$
		2ν	g.s.-2^+ (1293.5 keV)	$\geqslant 0.6(1.1)\times 10^{21}$
		2ν	g.s.-0_1^+ (1756.8 keV)	$\geqslant 0.8(2.2)\times 10^{21}$
		2ν	g.s.-0_2^+ (2027.3 keV)	$\geqslant 0.4(0.6)\times 10^{21}$
^{180}W	2ε	0ν	g.s.-g.s.	$\geqslant 0.9(1.3)\times 10^{17}$
	$2K$	2ν	g.s.-g.s.	$\geqslant 0.7(0.8)\times 10^{17}$
^{186}W	$2\beta^-$	0ν	g.s.-g.s.	$\geqslant 1.1(2.1)\times 10^{21}$
		0ν	g.s.-2^+ (137.2 keV)	$\geqslant 1.1(2.0)\times 10^{21}$
		$0\nu M1$	g.s.-g.s.	$\geqslant 1.2\ (1.4)\times 10^{20}$
	$2\beta^-$	2ν	g.s.-g.s.	$\geqslant 3.7(5.3)\times 10^{18}$
		2ν	g.s.-2^+ (137.2 keV)	$\geqslant 1.0(1.3)\times 10^{19}$

$= 0.012$; etc. The fit of the energy spectrum of Fig. 10 in the energy interval 2.2–3.4 MeV gives the area of the peak searched for as $S=-1.0\pm 1.6$ counts. The latter leads, for example, to the half-life limit on the $0\nu 2\varepsilon$ capture in ^{106}Cd: $T_{1/2}^{0\nu 2\varepsilon}(\text{g.s.}\rightarrow\text{g.s.})\geqslant 0.8(1.7)\times 10^{19}$ yr at 90% (68%) C.L. In the same way, restrictions on the other 0ν and 2ν double β decays in ^{106}Cd were derived and they are listed in Table III.

IV. DISCUSSION AND CONCLUSIONS

All half-life limits on 2β decay processes obtained in the present experiment with the help of the low background $^{116}CdWO_4$ scintillators are summarized in Table III. It should be stressed that most of the bounds for ^{106}Cd, ^{108}Cd, ^{114}Cd, ^{116}Cd, ^{180}W, and ^{186}W are higher than the previous results or have been established for the first time. For example, the limit $T_{1/2}^{0\nu}\geqslant 10^{21}$ yr on the $0\nu 2\beta$ decay of ^{186}W is nearly one order of magnitude higher than the previous one [25], while the bounds for the 0ν decay with Majoron emission and for the 2ν decay to the first (2^+) excited level of ^{186}Os were set for the first time. Note that up to now the level of sensitivity $T_{1/2}^{0\nu}\geqslant 10^{21}$ yr was reached only for ten nuclides [8]. Nevertheless, the obtained results are still far from the theoretical predictions, which, e.g., for the $0\nu 2\beta$ decay of ^{186}W are in the range of 6×10^{24} yr [47]–5×10^{25} yr [48] (for $m_\nu = 1$ eV), thus further efforts in this direction would be needed.

Besides, in the course of the present experiment two important by-products were obtained: (i) the half-life ($T_{1/2}=7.7^{+0.3}_{-0.3}\times 10^{15}$ yr) and the spectrum shape of the fourth-forbidden β decay of ^{113}Cd were measured [35]; (ii) indication for the α decay of ^{180}W with a half-life $T_{1/2}^{\alpha}=1.1^{+0.9}_{-0.5}\times 10^{18}$ yr has been observed for the first time, and new $T_{1/2}$ bounds were set for α decay of ^{182}W, ^{183}W, ^{184}W, and ^{186}W at the level of 10^{20} yr [33].

As regarding the main results of the present experiment on the 2β decay of ^{116}Cd, note that the refined half-life value of the two-neutrino 2β decay of ^{116}Cd is measured as

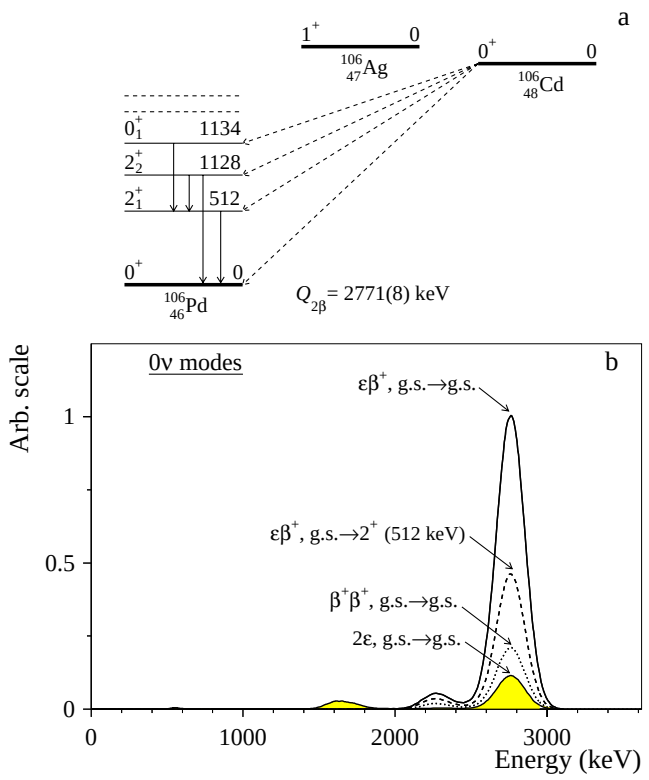

FIG. 11. (a) (Color online) The level scheme of the ^{106}Cd-^{106}Ag-^{106}Pd triplet. (b) Simulated response functions of the $^{116}CdWO_4$ detector to different 0ν modes of the 2β decay processes in ^{106}Cd.

$T^{2\nu}_{1/2} = 2.9^{+0.4}_{-0.3} \times 10^{19}$ yr. The experimental $2\nu2\beta$ Kurie plot is well described by a straight line, and the derived $Q_{\beta\beta}$ value (2808 ± 43 keV) is in accordance with the table value 2805(4) keV.

It should be noted that all half-life limits obtained here for ^{116}Cd are the most stringent for that nucleus, as for example, the bound on half-life of the $0\nu2\beta$ decay of ^{116}Cd (g.s. $\rightarrow$g.s.):

$$T^{0\nu}_{1/2} \geqslant 1.7(2.6) \times 10^{23} \text{ yr at } 90\%(68\%)\text{C.L.}$$

Using this bound and calculations [47], one can derive restrictions on the Majorana neutrino mass and right-handed admixtures in the weak interaction: $m_\nu \leqslant 1.9$ eV, $\eta \leqslant 2.5 \times 10^{-8}$, $\lambda \leqslant 2.2 \times 10^{-6}$ at 90% C.L. Neglecting right-handed contribution we get $m_\nu \leqslant 1.7$ (1.4) eV at 90% (68%) C.L., and on the basis of [42] the limit is $m_\nu \leqslant 1.5$ (1.2) eV. These results together with the best $T^{0\nu}_{1/2}$ limits obtained in the most sensitive direct experiments (and the corresponding restrictions on the Majorana neutrino mass) are given in Table IV. The m_ν constraints are determined on the basis of the calculations of Ref. [47], which were chosen because of the extensive list of 2β candidate nuclei calculated in this work, which allows one to compare the sensitivity of different experiments to the m_ν bound within the same scale.

It is obvious from Table IV that our experimental result on ^{116}Cd is one of the best after those based on ^{76}Ge studies and offers the restriction on the neutrino mass at the level of ≈ 1.5 eV similar to those of experiments with ^{130}Te and ^{136}Xe. In accordance with Ref. [50] the value of the R-parity violating parameter of minimal SUSY standard model is restricted by our $T^{0\nu}_{1/2}$ limit to $\varepsilon \leqslant 7.0(6.3) \times 10^{-4}$ at 90% (68%) C.L. (calculations [51] give more stringent restrictions: $\varepsilon \leqslant 2.7(2.4) \times 10^{-4}$). Moreover, using our bound on the $0\nu2\beta$ decay with one Majoron emission: $T^{0\nu}_{1/2} \geqslant 0.8(1.8) \times 10^{22}$ yr at 90% (68%) C.L. and calculations [52] the effective Majoron-neutrino coupling constant can be restricted to $g_M \leqslant 8.1(5.4) \times 10^{-5}$, and on the basis of calculation [42] to $g_M \leqslant 4.6(3.1) \times 10^{-5}$, which are among the strongest constraints obtained up to date in the direct 2β decay experiments with ^{76}Ge, ^{82}Se, ^{100}Mo, ^{130}Te, and ^{136}Xe [8].

We consider the Solotvina experiment on the 2β decay of ^{116}Cd as a pilot study for the future large scale project CAMEO [53], which intends to operate ≈ 100 kg of enriched $^{116}CdWO_4$ crystals allocated in the liquid scintillator of the BOREXINO Counting Test Facility. Results of our measurements with ^{116}Cd and Monte Carlo simulations evidently show that sensitivity (in terms of the half-life limit for the $0\nu2\beta$ decay) of the CAMEO experiment with 100 kg of enriched $^{116}CdWO_4$ crystals is of the order of 10^{26} yr [53]. The last value corresponds to a limit on the neutrino mass $m_\nu \leqslant 0.06$ eV, which would be of great interest for the modern physics.

TABLE IV. The best reported $T^{0\nu}_{1/2}$ and m_ν limits from direct 2β decay experiments.

Nuclide	Experimental limit $T^{0\nu}_{1/2}$ (yr)		Reference	Limit on m_ν (eV) on the basis of Ref. [47]	
	68% C.L.	90% C.L.		68% C.L.	90% C.L.
^{76}Ge	3.1×10^{25}	1.9×10^{25}	[18]	0.27	0.35
		1.6×10^{25}	[19]		0.38
	4.2×10^{25} [a]	2.5×10^{25} [a]	[49]	0.24	0.31
^{116}Cd	2.6×10^{23}	1.7×10^{23}	Present work	1.4	1.7
^{130}Te		2.1×10^{23}	[16]		1.5
^{136}Xe		4.4×10^{23}	[17]		2.2

[a]Results were established [49] by analyzing the cumulative datasets of the Heidelberg-Moscow [18] and IGEX [19] experiments.

ACKNOWLEDGMENTS

The authors express their gratitude to V.N. Kuts, V.V. Muzalevsky and S.S. Nagorny, who have contributed to the development, preparation, and fulfillment of the Solotvina experiment at its different stages. We would also like to thank the staff of the Solotvina Underground Laboratory, in particular, M.S. Sheichuk and D.Yu. Sedlak for the technical support of the measurements. One of us (F.A.D.) wishes to thank the INFN Sezione di Firenze for support during his several stays in Firenze.

[1] Y. Fukuda *et al.*, Super-Kamiokande Collaboration, Phys. Rev. Lett. **81**, 1562 (1998); **82**, 1810 (1999); **82**, 2430 (1999); **86**, 5651 (2001).
[2] Q.R. Ahmad *et al.*, SNO Collaboration, Phys. Rev. Lett. **87**, 071301 (2001); **89**, 011301 (2002); **89**, 011302 (2002).
[3] K. Eguchi *et al.*, KamLAND Collaboration, Phys. Rev. Lett. **90**, 021802 (2003).
[4] M.H. Ahn *et al.*, Phys. Rev. Lett. **90**, 041801 (2003).
[5] J.D. Vergados, Phys. Rep. **361**, 1 (2002).
[6] Yu.G. Zdesenko, Rev. Mod. Phys. **74**, 663 (2002).
[7] S.R. Elliott and P. Vogel, Annu. Rev. Nucl. Part. Sci. **52**, 115 (2002).
[8] V.I. Tretyak and Yu.G. Zdesenko, At. Data Nucl. Data Tables **80**, 83 (2002).
[9] R.K. Bardin *et al.*, Nucl. Phys. **A158**, 337 (1970); V.B. Brudanin *et al.*, Phys. Lett. B **495**, 63 (2000).
[10] A.A. Klimenko *et al.*, Nucl. Instrum. Methods Phys. Res. B **17**, 445 (1986); A. De Silva *et al.*, Phys. Rev. C **56**, 2451 (1997).
[11] F.A. Danevich *et al.*, Nucl. Phys. **A694**, 375 (2001).
[12] F.A. Danevich *et al.*, Nucl. Phys. **A717**, 129 (2003).
[13] S.R. Elliott *et al.*, Phys. Rev. C **46**, 1535 (1992).
[14] H. Ejiri *et al.*, Phys. Rev. C **63**, 065501 (2001).
[15] F.A. Danevich *et al.*, Phys. Rev. C **62**, 045501 (2000).
[16] C. Arnaboldi *et al.*, Phys. Lett. B **557**, 167 (2003).
[17] R. Luescher *et al.*, Phys. Lett. B **434**, 407 (1998).
[18] H.V. Klapdor-Kleingrothaus *et al.*, Eur. Phys. J. A **12**, 147 (2001).
[19] C.E. Aalseth *et al.*, Phys. Rev. C **59**, 2108 (1999); Phys. Rev. D **65**, 092007 (2002).
[20] Yu. G. Zdesenko *et al.*, in *Proceedings of the Second International Symposium on Underground Physics, Baksan Valley, 1987*, edited by G.V. Domogatsky (Nauka, Moscow, 1988), p. 291.
[21] F.A. Danevich *et al.*, Pis'ma Zh. Eksp. Teor. Fiz. **49**, 417 (1989) [JETP Lett. **49**, 476 (1989)].
[22] Yu.G. Zdesenko, J. Phys. G **17**, s243 (1991).
[23] F. A. Danevich *et al.*, in *Proceedings of the Third International Symposium on Weak and Electromagnetic Interaction in Nuclei (WEIN-92), Dubna, Russia, 1992*, edited by Ts.D. Vylov (World Scientific, Singapore, 1993), p. 575.
[24] F.A. Danevich *et al.*, Phys. Lett. B **344**, 72 (1995).
[25] A.Sh. Georgadze *et al.*, Yad. Fiz. **58**, 1170 (1995) [Phys. At. Nucl. **58**, 1093 (1995)].
[26] F.A. Danevich *et al.*, Nucl. Phys. B (Proc. Suppl.) **48A** , 232 (1996).
[27] F.A. Danevich *et al.*, Nucl. Phys. **A643**, 317 (1998).
[28] F.A. Danevich *et al.*, Nucl. Phys. B (Proc. Suppl.) **70A**, 246 (1999).
[29] P.G. Bizzeti *et al.*, Nucl. Phys. B (Proc. Suppl.) **110A**, 389 (2002).
[30] A.Sh. Georgadze *et al.*, Prib. Tekh. Éksp. **3**, 48 (1996) [Instrum. Exp. Tech. **39**, 191 (1996)].
[31] S.Ph. Burachas *et al.*, Nucl. Instrum. Methods Phys. Res. A **369**, 164 (1996).
[32] T. Fazzini *et al.*, Nucl. Instrum. Methods Phys. Res. A **410**, 213 (1998).
[33] F.A. Danevich *et al.*, Phys. Rev. C **67**, 014310 (2003).
[34] E. Gatti and F. De Martini, *Nuclear Electronics 2* (IAEA, Vienna, 1962), p. 265.
[35] F.A. Danevich *et al.*, Yad. Fiz. **59**, 5 (1996) [Phys. At. Nucl. **59**, 1 (1996)].
[36] *Table of Isotopes*, 8th ed. edited by R. B. Firestone *et al.* (Wiley New York, 1996).
[37] CERN Program Library Long Write-Up W5013, 1994.
[38] O.A. Ponkratenko *et al.*, Yad. Fiz. **63**, 1355 (2000) [Phys. At. Nucl. **63**, 1282 (2000)].
[39] F. A. Danevich *et al.* (unpublished).
[40] G. Audi and A.H. Wapstra, Nucl. Phys. **A595**, 409 (1995).
[41] H. Ejiri *et al.*, J. Phys. Soc. Jpn. **64**, 339 (1995).
[42] R. Arnold *et al.*, Z. Phys. C **72**, 239 (1996).
[43] G.J. Feldman and R.D. Cousins, Phys. Rev. D **57**, 3873 (1998).
[44] K. Hagiwara *et al.*, Phys. Rev. D **66**, 010001 (2002).
[45] R.N. Mohapatra *et al.*, Phys. Lett. B **491**, 143 (2000).
[46] K.J.R. Rosman and P.D.P. Taylor, Pure Appl. Chem. **70**, 217 (1998).
[47] A. Staudt *et al.*, Europhys. Lett. **13**, 31 (1990).
[48] J.G. Hirsch, O. Castanos, and P.O. Hess, Nucl. Phys. **A582**, 124 (1995).
[49] Yu.G. Zdesenko *et al.*, Phys. Lett. B **546**, 206 (2002).
[50] M. Hirsch *et al.*, Phys. Rev. D **53**, 1329 (1996).
[51] A. Faessler *et al.*, Phys. Rev. D **58**, 115004 (1998).
[52] M. Hirsch *et al.*, Phys. Lett. B **372**, 8 (1996).
[53] G. Bellini *et al.*, Phys. Lett. B **493**, 216 (2000); Eur. Phys. J. C **19**, 43 (2001).